Heliyon 5 (2019) e02415

Contents lists available at ScienceDirect

Heliyon

journal homepage: www.heliyon.com

Silver/quartz nanocomposite as an adsorbent for removal of mercury (II) ions from aqueous solutions

Rasha S. El-Tawil [a], Shaimaa T. El-Wakeel [b], Ashraf E. Abdel-Ghany [a], Hanaa A.M. Abuzeid [a], Khaled A. Selim [c], Ahmed M. Hashem [a,*]

[a] National Research Centre, Inorganic Chemistry Department, 33 El Bohouth St., (former El Tahrir St.), Dokki-Giza, 12622, Egypt
[b] National Research Centre, Water Pollution Research Department, Environmental Research Division, 33 El Bohouth St., (former El Tahrir St.), Dokki-Giza, 12622, Egypt
[c] Central Metallurgical Research & Development Institute, Minerals Technology Department, CMRDI, Cairo, Egypt

ARTICLE INFO

Keywords:
Environmental science
Silver nanoparticles (AgNPs)
Quartz
Nanocomposite
Adsorbent
Mercury (II)

ABSTRACT

Silver nanoparticles (AgNPs) and silver/quartz nanocomposite (Ag/Q)NPs)) were synthesized by sol-gel method using table sugar as chelating agent. The synthesized nanosized materials were used for mercury ions adsorption from aqueous solutions. The materials were characterized by X-ray diffraction (XRD), Transmission Electron microscope (TEM), and surface area (BET). Adsorption of Hg^{2+} (10 mg/l) is strongly dependent on time, initial metal concentration, dose of adsorbent and pH value. Silver/quartz nanocomposite ((Ag/Q)NPs)) shows better efficiency than individual silver nanoparticles (AgNPs). This composite removed mercury ions from the aqueous solution with efficiency of 96% at 60 min with 0.5g adsorbent dosage at pH 6. The adsorption process explained well by the pseudo-second-order kinetic model. In conclusion silver/quartz nanocomposite (Ag/Q)NPs)) shows higher removal efficiency for mercury ions from aqueous solutions than individual silver naoparticles (AgNPs) or quartz (Q).

1. Introduction

Clean water is a vital demand and basic necessity for human being [1, 2]. There is a shortage in clean water resources, almost one-sixth of the world's population suffers from this crisis [3]. This crisis comes from fast increase in world population, global warming and of course rapid dwindling of water resources. So, organized usage of water resources and reuse of treated wastewater using cheap and environmental friendly technologies is an effective way of conserving the limited resources of freshwater [4, 5]. Heavy metals in water sources cause severe health problems in animals, aquatic organisms and human beings through the food chain due to their high toxicity and non-biodegradable properties [6]. These pollutants resulted from elevated release of effluents by various industries such as plating, metallurgical, leather, metal finishing, welding alloy manufacturing plants, fertilizers, chemicals etc. [7, 8]. Mercury represents one of the largest levels of toxicity which can accumulate in ecosystems as listed by the World Health Organization (WHO) [9, 10]. Inorganic divalent mercury (Hg^{2+}) is discharged into ecosystem from different industries as paper and pulp, plastic, paints, battery, pharmaceutical and oil refineries. This toxic metal can damage the kidney, brain, reproductive and respiratory system [11, 12]. The high risk of mercury pushed researchers to search for various techniques for protection of environment and human beings through different remediation processes [13]. Several techniques e.g., filtration, chemical precipitation, solvent extraction, ion exchange, electrochemical deposition, electrolysis, and membrane process have been designed. Most of these methods are either expensive or inefficient for lower concentration of the heavy metal ion [14]. The adsorption method which is one of the most suitable, simple and economically techniques used to purify water and wastewater [15, 16, 17]. Several adsorbents have been applied to remove mercury ions such as clays, silica, carbon nanotubes, polymers and activated carbons [18, 19, 20, 21, 22, 23]. The nanosized metals or metal oxides have received great attention as adsorbents in water remediation due to their higher performance and lower cost than traditional old materials [24]. The nanomaterials have not only high surface area and hence high density of active sites per unit mass, but also high surface free energy, resulting in enhanced surface reactivity [25, 26, 27]. Metallic nanoparticles such as silver nanoparticles (AgNPs) have good behavior as viable adsorbents as they have good chemical and physical properties. Ag NPs have high catalytic activity, biocompatibility, high adsorption

* Corresponding author.
E-mail address: ahmedh242@yahoo.com (A.M. Hashem).

https://doi.org/10.1016/j.heliyon.2019.e02415
Received 21 January 2019; Received in revised form 9 April 2019; Accepted 30 August 2019

capacity due to its high surface area and can be reused and separated easily [28, 29]. Some studies on removal of mercury have used silver nanoparticles as adsorbents [30, 31]. As the chemically synthesized AgNPs have low adsorption capacity due to its lower stability and its tendency to be aggregated, an urgent appropriate synthesis technique for the development of stable silver is required [4]. AgNPs may be stabilized by mixing with other inorganic metal oxides e.g. SiO_2, TiO_2, ZnO, SiO_2-TiO_2 forming composite nanoparticles of silver-metal oxides [32, 33, 34, 35, 36]. Quartz sand, which is the main component of natural sand stone is used widely in industrial manufactories due to its physical and chemical characteristics such as low cost, resistant to high temperature and non-toxic [37, 38, 39]. There was no great attention to the use of quartz sand as a natural adsorbent to remove heavy metals from water. For the above reason, this study will focus on using AgNPs/quartz (Ag/Q) nanocomposite as an adsorbent to remove mercury from aqueous solution by sol-gel method, considered as a versatile and cheap technique. Table sugar was used as chelating agent to prepare AgNPs then modified by quartz to prepare AgNPs/quartz composite. The samples prepared were characterized by X-ray diffraction (XRD), transmission electron microscopy (TEM), and surface area (BET). The efficiency of the prepared sample for efficient removal of Hg^{2+} from aqueous solution was explored at different operating conditions such contact time, initial metal concentration, initial pH and adsorbent dosage. The experimental data were fitted with various kinetic and isotherm models to explain the adsorption mechanism.

2. Materials and methods

2.1. Materials

All the reagents used were of analytical grade and used directly as received and stock solutions were prepared using deionized water. Pure $AgNO_3$ (Aldrich, Germany) and table sugar were used to prepare silver nanoparticles. Pure quartz samples were purchased from El-Nasr Mining Company to prepare a composite of silver/quartz nanoparticles (Ag/Q) NPs). To prepare the working mercury stock solution for the adsorption experiments, Pure $Hg(NO_3)_2$ (Aldrich, Germany) was used.

2.2. Synthesis and characterization of Ag/quartz (Ag/Q)NPs composite nanoparticles

In this study silver nanoparticles (AgNPs) and composite of (Ag/Q) NPs were prepared using sol-gel technique assisted by table sugar as chelating agent. Silver nanoparticles were prepared by dissolving 4.724g of $AgNO_3$ in bidistilled water to prepare $AgNO_3$ solution. The solution was added drop wisely to 1.5 M solution of table sugar. The entire solution was heated at 80 °C till evaporation and formation a black gel. The collected zero-gel was dried overnight at 90 °C then calcined at 350 °C for 5 hours in an ambient atmosphere yielded powder of silver nanoparticles. The same procedure mentioned above has been used to prepare silver-quartz composite (Ag/Q)NPs. Simply calculated and intended amount of quartz was dropped in the sol-solution of Ag salt and table sugar. The entire mixture was heated until formation of a gel. The collected zero-gel was dried overnight at 90 °C then calcined at 350 °C for 5 hours in an ambient atmosphere yielded composite of silver/quartz nanoparticles.

Different techniques characterized the synthesized samples. X-ray powder diffraction patterns (XRD) were recorded using a Philips X'Pert apparatus equipped with a CuKα X-ray source (λ = 1.54056 A°) in the 2θ range 10–80°. Transmission electron microscope, JEOL (TEM, JEM-1230) Japan used for investigation the morphology of prepared samples. The specific surface area was measured by nitrogen adsorption/desorption at 77 K using BET method (Quantachrome NOVA Automated Gas Sorption). The concentrations of Hg^{2+} were measured using inductively coupled plasma optical emission spectrometry (ICP-OES) (Agilent 5100) according to APHA 2012. Finally, mercury ions removal from wastewater using silver-quartz composite nanoparticles was studied using multiple batch sets of experiments.

2.3. Adsorption study

All batch adsorption experiments were conducted by mixing an sufficient amount of adsorbents (silver nanoparticles (AgNPs), quartz (Q) and silver-quartz composite nanoparticles (Ag/Q)NPs)) with a known volume of Hg^{2+} at varoius initial concentrations (5, 10, 50 and 100 mg/l) with shaking (150 r/min). Then, the supernatants were separated from the mixture solution by filtration with PTEF syringe filter. The influence of contact time was assessed at different time intervals by agitation (5–150 min). In order to optimize the adsorption process, other factors such as initial pH, adsorbent dose (0.05–1 g) and temperature were also examined.

Based on the following equations, the equilibrium adsorption capacity, qe (mg/g) and the removal efficiency of metal ions were estimated:

$$q_{e} = (C_{\circ} - C_{e})\frac{V}{m} \tag{1}$$

$$\%\ \text{Removal} = \frac{Ci - Ce}{Ci} \times 100 \tag{2}$$

Where V: sample volume (L), m: mass of the adsorbents (g), C_o: initial metal ion concentration (mg/L), and C_e: equilibrium concentration of metal ion in the solution (mg/L).

2.4. Adsorption isotherms, kinetics and thermodynamic studies

The equilibrium data, commonly known as adsorption isotherms are basic parameters for the design of adsorption systems and these data provide information on the adsorbent capacity or the amount required to remove a pollutant mass under the system conditions. The equilibrium adsorption isotherm data for Hg^{2+} adsorption by the prepared composite (Ag/Q)NPs) are fitted in different classical models. The Freundlich, Eq. (3) [40], Langmuir, Eq. (4) [41], Dubinin–Radushkevich, Eq. (5) [42] and Redlich– Peterson Eq. (6) [43] are the models used in this research to investigate the adsorption equilibrium

$$q_{e} = K_{F} C_{e}^{1/n} \tag{3}$$

$$q_{e} = q_{m} K_{L} \frac{C_{e}}{1 + K_{L} C_{e}} \tag{4}$$

$$q_{e} = q_{s}\, e^{\left(-K_{DR}\varepsilon^{2}\right)} \tag{5}$$

$$q_{e} = \frac{K_{R} C_{e}}{1 + a_{R} C_{e}^{g}} \tag{6}$$

Where, C_e (mg/L) is the equilibrium concentration, (k_F) and (n) are the Freundlich adsorption constants which are related to the adsorption capacity and intensity, respectively. 1/n is a function of the strength of adsorption in the adsorption process where, the smaller 1/n the greater the expected heterogeneity and it is a characteristic parameter of Freundlich isotherm. The value of $1/n < 1$ shows a normal adsorption, when $1/n > 1$ shows a cooperative adsorption, K_L (L/mg) is the Langmuir equilibrium constant related to the affinity of adsorption sites and q_e (mg/g) represents the maximum theoretical monolayer adsorption capacity. Langmuir isotherm based on homogeneous and monolayer adsorption while Freundlich isotherm deals with heterogeneous and multilayer adsorption process. The favorability of adsorption of Hg^{2+} ions was tested using a dimensionless constant separation factor or equilibrium constant (R_L) that is a characteristic parameter of Langmuir isotherm which defined based on Eq. (7):

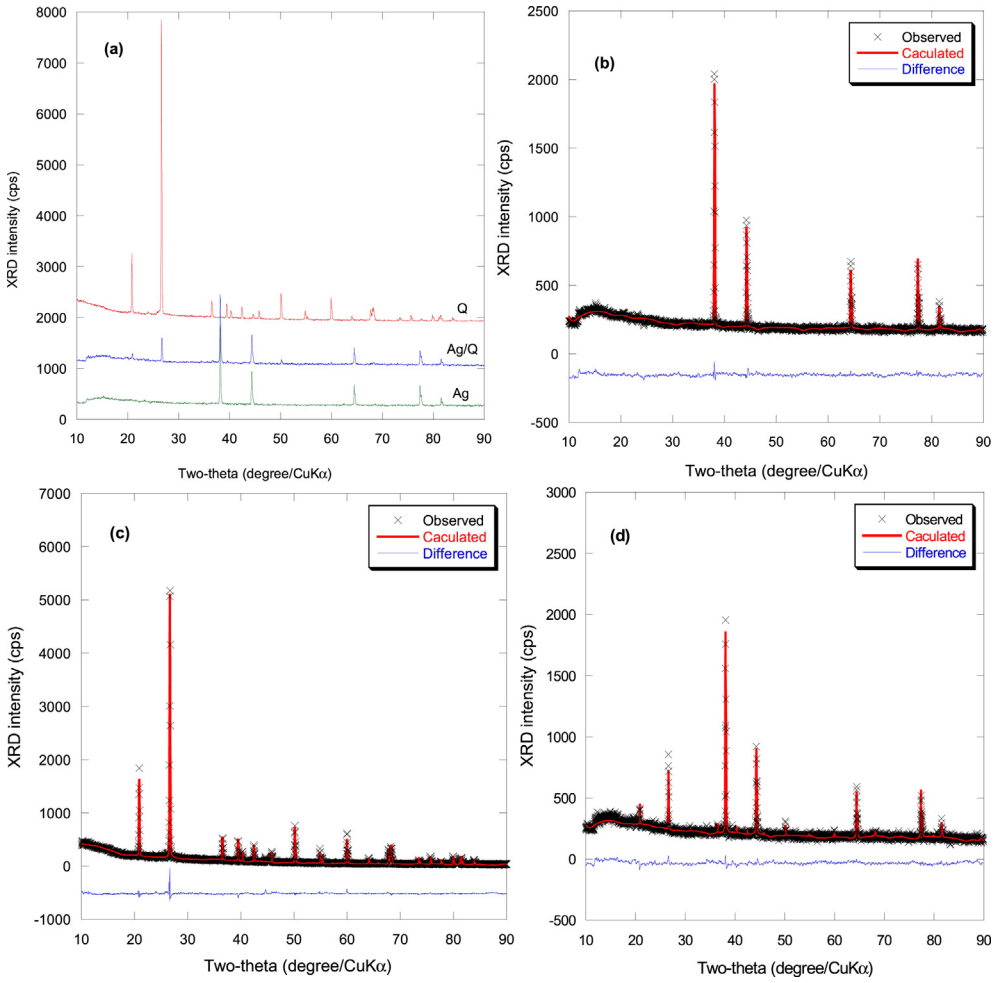

Fig. 1. (a) XRD pattern of AgNPs, Quartz and (Ag/Q)NPs) composite and Rietveld refinements of XRD patterns of (b) AgNPs, (c) Quartz and (d) (Ag/Q) NPs) composite.

$$R_L = \frac{1}{1 + bC_0} \tag{7}$$

The R_L value indicates whether the isotherm is favorable ($0 < R_L < 1$), unfavorable ($R_L > 1$), linear ($R_L = 1$), or irreversible ($R_L = 0$).

The Dubinin–Radushkevich isotherm model Eq. (5) was chosen to estimate the characteristic porosity of the adsorption process where, β is a constant related to mean free energy (mol^2/kJ^2), and ε representing Polanyi potential, which can be calculated from Eq. (8):

$$\varepsilon = RT\ ln\left(1 + \frac{1}{C_e}\right) \tag{8}$$

The isotherm formulated for the adsorption process following a pore filling mechanism by calculating its mean free energy, the apparent energy of adsorption E (kJ/mol) is calculated from β by the Eq. (9):

$$E = \frac{1}{\sqrt{-2\beta}} \tag{9}$$

Redlich-Peterson isotherm model has a linear dependence on concentration and represent adsorption equilibrium over a wide concentration range in homogeneous or heterogeneous systems. The isotherm approaches Freundlich isotherm model at high concentration (as the exponent β tends to zero) and is in accordance with the lower concentration limit of the ideal Langmuir condition (as the β values are all close to 1). k_R (L/mg) constant related to the adsorption capacity, a_R (L/mg) constant related to the affinity of the binding sites and g (g) exponent related to the adsorption intensity which lies between 0 and 1.

To investigate the adsorption mechanism its potential kinetic models have been exploited to analyze the experimental data. Adsorption kinetics were performed at different time intervals (5–120) and constant metal concentration (20 mg/l) at room temperature through adsorption experiments. Several kinetic models such as Pseudo-first-order Eq. (10) [44], pseudo-second-order Eq. (11) [45], and Intra-particle diffusion model Eq. (12) [46]:

Models are expressed in equations as follows:

$$q_t = \ q_e - \left(1 - e^{(-K_1 t)}\right) \tag{10}$$

$$q_t = \frac{K_2 q_e^2\ t}{1 + k_2 q_e\ t} \tag{11}$$

where, q_t: is the amount of adsorbed metal at equilibrium (mg/g) at time t and k_1 (min^{-1}), k_2 (g/mg.min) are the adsorption rate constants.

The pseudo-second-order model could not identify the diffusion mechanism and the kinetic results were then analyzed by using the intra-particle diffusion model. In the model developed by Weber and Morris [47], the initial rate of intra-particle diffusion is calculated by linearization of Eq. (12):

$$q_t = \ k_p t^{1/2} + \ C \tag{12}$$

where, C: is the intercept and k_p: is the intra-particle diffusion rate constant (mg/g $min^{1/2}$).

In any adsorption process, both energy and entropy considerations

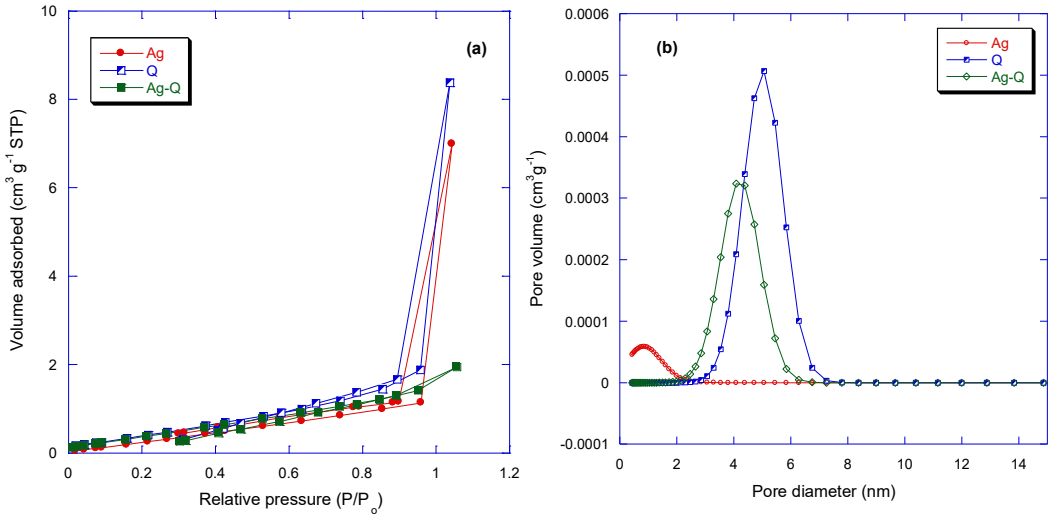

Fig. 2. (a) N_2 adsorption-desorption isotherms and (b) the pore size distribution (PSD) curves of (AgNPs), quartz and AgNPs/quartz composite.

must be taken into account in order to determine what process will occur spontaneously. Values of thermodynamic parameters are the actual indicators for practical application of a process. The effect of different temperatures (298, 313, 333 and 348 K) on Hg^{2+} adsorption was studied and the experimental data obtained were used in calculating the thermodynamic parameters as Gibbs free energy (ΔG°), the enthalpy change (ΔH°) and entropy change (ΔS°) which are determined according equations:

$$\Delta G^{\circ} = -RT\ln K_d \quad (13)$$

k_d is the distribution coefficient of the solute which is equal q_e/C_e, R is the ideal gas constant (8.314 J/mol K). The thermodynamic parameters were obtained using Van't Hoff equation [48].

$$\ln K_d = \frac{\Delta S}{R} - \frac{\Delta H}{RT} \quad (14)$$

$$\Delta G^{\circ} = \Delta H^{\circ} - T\Delta S^{\circ} \quad (15)$$

2.5. Leaching and regeneration studies

Leaching of Ag^+ ions from the prepared composite was determined by using the batch leaching test using distilled water. The test was performed at a ratio of 0.5 g/l at different stirring times (2,6,12,24,36 and 48 h). At the end of the leaching process, the samples were filtered and the concentration of Ag^+ ions were determined by means of ICP-OES (Agilent 5100). To study the regeneration ability of the adsorbent, the composite samples saturated with Hg^{2+} ions were conducted with different desorbing agents 0.1 M HNO_3, and HCl for 1h. After each cycle of sorption/desorption, the solution was washed with deionized water to reach to neutral pH and then the adsorbent was dried for reuse in the next cycle. The concentrations of Hg^{2+} and Ag^+ were monitored in each cycle.

3. Results and discussion

3.1. Structural characterization

The crystal structures of silver nanoparticles (AgNPs), quartz and its composite (Ag/Q)NPs) are analyzed by X-ray diffraction and displayed in Fig. 1a and their refined X-ray diffraction patterns are reported in Fig. 1 b–d. XRD and refined XRD of AgNPs and quartz shown in Fig. 1 a–c displayed well indexed XRD peaks for AgNPs of cubic structure with space group Fm*3m* (JCPDS file 03-0931). These figures confirmed also, the trigonal structure with space group *P3221* (JCPDS file 46-1045) for quartz. So, pure phases of AgNPs and quartz are obtained without impurity peaks. Refined XRD result of AgNPs/quartz composite (Ag/Q)NPs) is shown in Fig. 1d. The composite still has the crystalline state. Strong and sharp diffraction lines originate from silver (Ag) with a cubic structure (*Fm3m*) and quartz with a trigonal structure (*P3221*). From the beginning we aimed to fabricate 50:50 % of AgNPs/quartz composite. Rietveld refinement of this composite detected 46.8: 53.2% of AgNPs/quartz close to the starting ratio that we used. A slight decrease in the net area and intensity of silver and quartz diffraction lines corresponds to a decrease of silver and quartz amounts from 100% in each pure phase to 46.8 and 53.2%, respectively in the composite. In addition, quartz matrix enables incorporation of silver particles [49]. So, this quartz matrix acts as a shield and protects accommodated silver particles to be oxidized. Incorporation of AgNPs inside quartz matrix may provide not only new active centers in quartz matrix, but also a long adsorbent effect for removal of toxic heavy metals. There is no evidence in the XRD spectrum for Ag_2O or other silver oxides, as compared with reported data [50, 51]. This clearly shows that stable Ag nanoparticles could be fabricated with quartz composite.

Table 1
The porous structural data of of (AgNPs), quartz and (Ag/Q)NPs composite.

Sample	BET surface Area ($m^2.g^{-1}$)	Total pore volume ($cm^3.g^{-1}$)	Average pore size (nm)
AgNPs	138	0.0051	14.76
quartz	188	0.0070	14.78
(Ag/Q) NPs	172	0.0031	5.78

Fig. 2a and b, show the nitrogen adsorption–desorption isotherms and pore-size distributions (PSD) for the pure AgNPs, quartz and (Ag/Q)NPs) composite, respectively. All the three samples exhibit similar shape of the isotherms that can be described as type II and H3 hysteresis loop under the IUPAC-classification [52, 53], implying the presence of porous structure [27, 54]. The analysis of the pore distribution in Fig. 2b showed that the pores distribution for all three samples is very uniform. For (Ag/Q)NPs) composite, The shift in the distribution of pores to small pores can be attributed to the presence of some silver nanoparticles within the pure quartz host matrix [55]. This phenomenon is also associated with a decrease in BET surface area. Based on the isotherms (Fig. 2a), the isotherms for the (Ag/Q)NPs) composite is similar in shape to the pure AgNPs and quartz. The BET surface area, the total pore

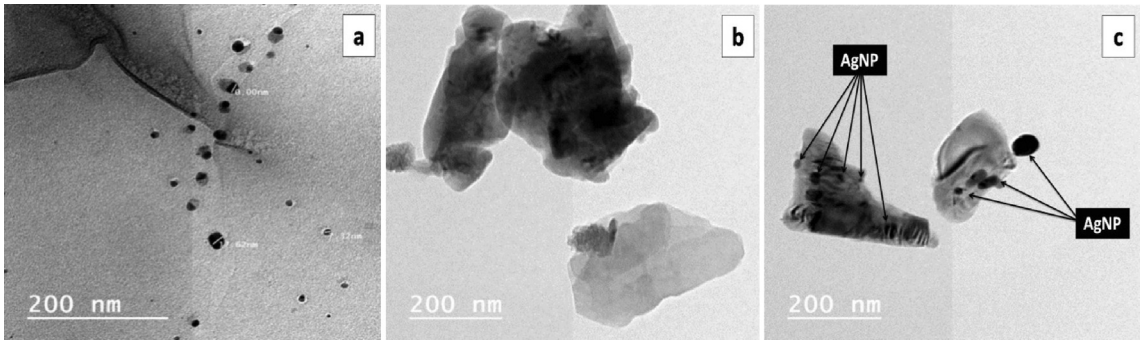

Fig. 3. TEM images of (a) AgNPs, (b) Quartz and (c) (Ag/Q)NPs) composite.

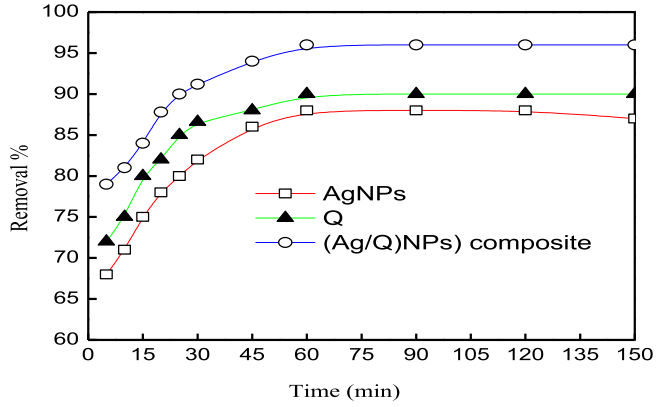

Fig. 4. Effect of contact time on the removal of Hg^{2+} by the prepared materials (adsorbent dose = 1g, initial concentration 10 ppm).

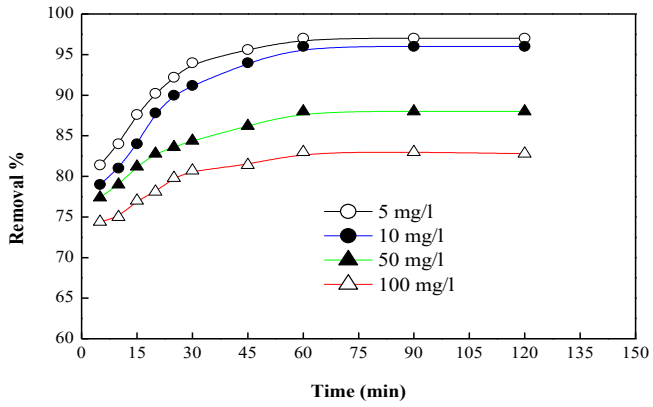

Fig. 5. Effect of contact time and initial concentration on the removal of Hg^{2+} by (Ag/Q)NPs) composite (adsorbent dose = 1g, agitation speed: 200 rpm, initial metal concentration: 5,10, 50,100 mg/L).

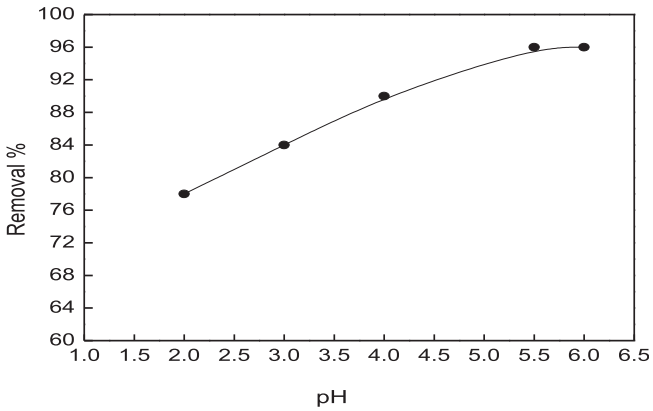

Fig. 6. Effect of pH on the removal of Hg^{2+} by (Ag/Q)NPs) composite (amount of adsorbent: 1 g; agitation speed: 200 rpm, initial metal concentration: 10 mg/L).

volume and the porosity of the (Ag/Q)NPs) composite are smaller than that obtained for the pure AgNPs and quartz (Table 1). This can be due to the dispersion of Ag nanoparticles inside the mesoporous quartz and decrease the degree of porosity of quartz, but increase the active adsorbent sites of composite as we will notice in adsorption activity of composite for removal of Hg.

Transmission electron microscopy (TEM) has been employed to characterize the size, shape and morphology of silver nanoparticles (AgNPs), quartz and (Ag/Q)NPs) composite as shown in Fig. 3 (a–c). Fig. 3a shows that AgNPs are spherical in shape having smooth surface and are well dispersed. TEM image also show that the AgNPs having different size distributions between 12-60nm. The minimum and maximum size of AgNPs are about 12 and 60 nm respectively, the large particles size may be due to aggregation or clustering of the Ag nanoparticle. The average diameter of AgNPs is found to be approximately 25nm. TEM images of pure quartz (Fig. 3b) show irregular, big and non-homogeneous particles. TEM of (Ag/Q)NPs) composite is shown in Fig. 3c, the nanocomposite consists of AgNPs not only located on the surface but also embedded within the matrix of quartz.

3.2. Adsorption studies

Contact time and concentration dependence sorption of Hg^{2+} was studied within a wide range of initial concentrations using the examined adsorbents. Fig. 4 shows the removal efficiency of Hg^{2+} ions with time by AgNPs, quartz and (Ag/Q)NPs) composite at initial metal concentration of 10 mg/L. The removal of Hg^{2+} in the first 30 min attained 82%, 86.5% using AgNPs and Q respectively while (Ag/Q)NPs) composite removed 92.1% of Hg^{2+} ion at the same time (30 min). The adsorption attained an apparent equilibrium at 60 min with a removal percentage of 96 % using (Ag/Q)NPs) composite, while, the adsorbed Hg^{2+} remained constant. Further increase of contact time does not significantly affect the Hg^{2+} adsorption capacity due to the saturation of the active binding sites. By increasing the initial concentration of Hg^{2+} ions, the adsorption decreases as shown in Fig. 5. At low concentration, for few numbers of mercury ions to be adsorbed, more effective adsorption sites are available, but at higher concentration, the number of mercury ions is much higher than the available adsorption sites. The rivalry of mercury ions for response with the adsorbent surface is growing by raising the original concentration of mercury ions. As a consequence, more active adsorbent sites are saturated. Furthermore, the amount of collisions between mercury ions and adsorbents is increasing and adsorption is increasing [56]. The adsorption efficiency reached 97, 96, 88 and 83 % using 5, 10, 50,

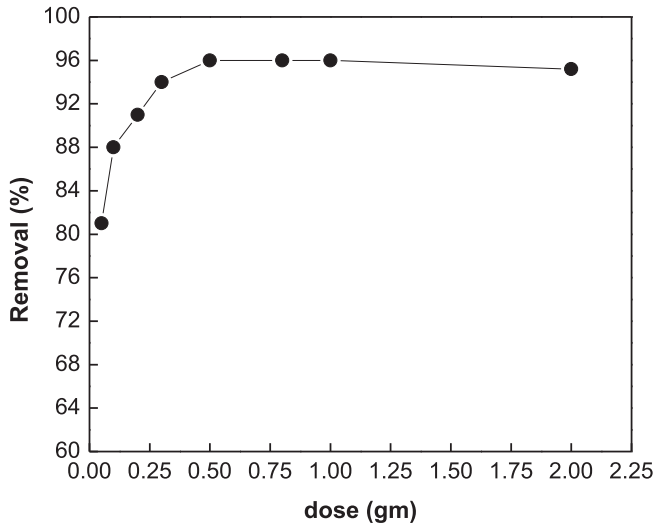

Fig. 7. Effect of adsorbent dose on the removal of Hg^{2+} by (Ag/Q)NPs) composite (agitation speed: 200 rpm, initial metal concentration: 10 mg/L).

Table 2
Adsorption isotherm models parameters of Hg^{2+} adsorption by (Ag/Q)NPs composite.

Isotherm models	Parameters	
Freundlich model	K_F(L/g)	62 ± 12
	n	2.8 ± 0.3
	R^2	0.94
Langmuir model	q_m(mg/g)	376.3 ± 17
	K_L(L/mg)	0.06 ± 0.01
	R^2	0.98
Dubinin-Radushkevich model	q_s(mg/g)	320 ± 29
	K_{DR}(L/mg)	1.97 × 10^{-6} ± 6.9
	E (KJ/mol)	11.7
	R^2	0.826
Redlich–Peterson model	R^2	0.89±
	K_R (L/mg)	26.8±1.3
	a_R (L/mg)	0.072±0.009
	g (g)	1±0.01

100 mg/l respectively. The equilibrium time of adsorption is independent of initial concentrations. Slight differences in removal percentage obtained between initial concentrations of 5 and 10 mg/l.

The effect of pH is a significant factor in the process of metals adsorption from aqueous solution. The influence of pH on mercury ions removal by the (Ag/Q)NPs) composite in the pH range of 2–6 is given in Fig. 6 at the optimum time 60 min. The increase in removal percentage was observed till reached the maximum removal at pH 6. In addition, mercury ions are free of Hg^{2+} at pH less than 6 and positively charged hydrogen ions compete with Hg^{2+} for binding with adsorbent active sites on the surface of (Ag/Q)NPs composite. If the composite adsorbent surface (Ag/Q)NPs) is protonated by hydrogen ions, the electrostatic interaction will reduce and the effectiveness of Hg^{2+} adsorption by the composite (Ag/Q)NPs will reduce. At pH up to 6, metal removal improved owing to the reduction in rivalry for the same functional groups between proton and metal cation. Hg^{2+} particles start depositing as hydroxides $Hg(OH)_2$ or soluble $Hg(OH)^+$ at pH more than 6 [57,55]. The studies were therefore not carried out at pH more than 6 because the precipitates in the solution will be created. As consequence, this research regarded that the optimum pH was equivalent to 6.

The effect of (Ag/Q)NPs) composite dose on Hg^{2+} removal was investigated at 60 min and pH 6 for dose (0.05–1 g). Increasing the amount of adsorbing sites available results in enhanced adsorbent effectiveness in removing ions from mercury to a certain limit. After this limit and at elevated adsorbent dose, the level of mercury in solution

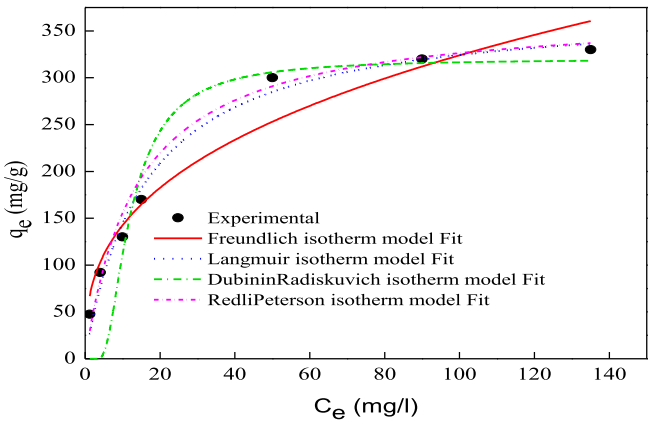

Fig. 8. Freundlich, Langmuir, Dubinin Radiskuvich and Redli-Peterson non-linear isotherm fitting models.

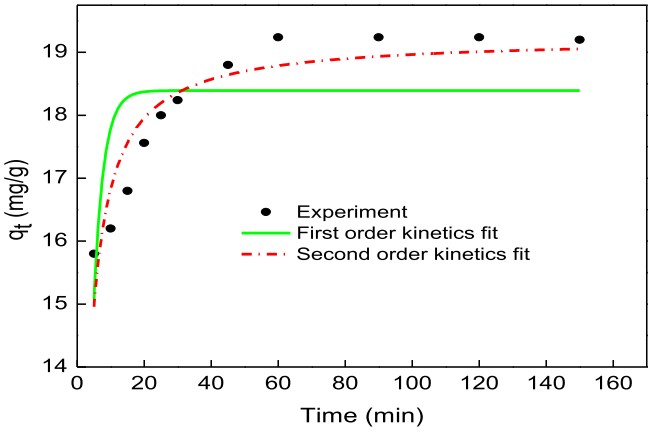

Fig. 9. Nonlinear fitting of Pseudo-first order and Pseudo-second order kinetics plots of Hg^{2+} ions adsorption onto (Ag/Q)NPs composite.

reaches a minimum quantity, and then the effectiveness of removing Hg^{2+} starts to decrease. This conduct is shown clearly in Fig. 7, Hg^{2+} ions removal percentage increased from 81% to 96% using 0.05 g and 0.5 g, respectively. The efficiency of removal using dose greater than 0.5 g showed no significant increase in removal of Hg^{2+}, so the optimum adsorbent dose was considered to be 0.5 g.

Using isothermic models (Langmuir Eq. (3), Freundlicheq.4, Dubinin–Radushkevich (D-R)Eq. (5) and Redlich–Peterson (R–P) eq.6) were evaluated to optimize the adsorption method. The experimental information were better fitted with the Langmuir model with correlation factor (R2) 0.98 as shown in Table 2 and Fig. 8. In this study the q_{max} value for Hg^{2+} ions adsorption on the nanocomposite was 376.2 mg g^{-1}. The values of R_L are ranged between 0.12 and 0.92 revealing that the adsorption is favorable. The value of (1/n) is 0.35 which less than unity indicating a favorable adsorption process of Hg^{2+} ions onto (Ag/Q)NPs composite and chemisorption reaction. The values of the apparent energy of adsorption E, obtained from D-R model is 11.7 kJ/mol that is between 8 and 16 kJ/mol revealing chemical ion exchange mechanism. The Redlich–Peterson isotherm showed the less fitting of the equilibrium data. The values of the applied isotherm parameters are listed in Table 2. The value of g in Redlich–Peterson isotherm is equal 1, indicating a favorable adsorption and the R–P equation can be reduced to the Langmuir equation. So, Langmuir is the most appropriate model describing the experimental data for Hg^{2+} adsorption.

Different kinetic adsorption models (Pseudo-first order, Pseudo-second order, and intra-particle diffusion) were used for Hg^{2+} ions adsorption on (Ag/Q)NPs composite in order to recognize the kinds of

Table 3
Adsorption kinetics models parameters of Hg^{2+} adsorption by (Ag/Q)NPs composite.

Kinetic models	Parameters	
First order model	q_e(mg/g)	18.3 ± 0.31
	k_1(min^{-1})	0.34 ± 0.06
	R^2	0.38
	$q_{e(}$experiment)	19.24
Second order model	q_e(mg/g)	19.2 ± 0.23
	k_2(mg/g/min)	0.036 ± 0.005
	R^2	0.977
Intraparticle diffusion model	K_p(mg/g $min^{1/2}$)	0.66
	C	14.3

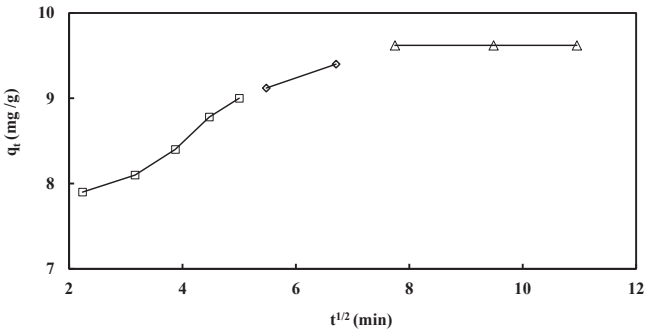

Fig. 10. Intraparticle diffusion kinetics of Hg^{2+} adsorption onto (Ag/Q) NPs composite (adsorbent dose: 0.5g, initial concentration:10 mg/l).

adsorption mechanism. Fig. 9 shows the nonlinear fitting of kinetic models of Hg^{2+} ions adsorption. Table 3 shows the estimated values for (qe) and the constants of the models. It can be seen that the value of the correlation coefficients (R2) acquired for the pseudo-first-order kinetic model Eq. (10) was small, which shows a poor linearization, and the estimated values (qe) collected from the plots were not compatible with the experimental values showing the adsorption by the pseudo-first-order kinetic model. The equation parameters of the pseudo-second order kinetic model Eq. (11) are shown in Table 3 and, as noted, the correlation coefficient (R2) was close to 1 and the calculated (qe) value was well agreed upon by the experimental value indicating that the response is well matched by pseudo-second order and that adsorption may happen through chemisorption response.

The kinetic data were analyzed by the intra-particle diffusion kinetic using Weber's equation Eq. (12) to explain the mechanism of chemical adsorption. The adsorption process may be controlled by film and pore diffusion (intra-particle diffusion), surface diffusion and adsorption on the pore surface [58]. The model is applied by plotting of qt vs. $t^{1/2}$ as shown in Fig. 10 and the parameters of the model are listed in Table 3. The plot should be linear if the adsorption follows a diffusion mechanism. The acquired plot shown in Fig. 10 did not pass through the origin and stated multi-step adsorption method which shows that not only intra-particle diffusion influenced adsorption by more than one method. The plot's original part stated external surface adsorption, while intra-particle or pore diffusion happened in the second part. The third part is ascribed to the final point of equilibrium, where intra-particle diffusion begins to slow down due or not to the exceptionally small levels of adsorbents in the solution. Mercurey ions removal mechanism is complicated as it involves adsorption, Hg^{2+} reduction to Hg° followed by surface precipitation and silver amalgam or alloy formation (Ag_xHg_y). This emerges from silver's affinity to form mercury amalgam. This hypothesis of the formation of silver amalgam was endorsed by Z. Tauanov et al. He used zeolite nanocomposite impregnated with carbon fly ash/silver NPs to remove Hg^{2+} from aqueous solution [59]. The mechanism of adsorption on the prepared nanocomposite may result from redox reaction of Ag°/Ag^{+} (+0.80 V) and Hg^{2+}/Hg° (+0.85 V), which

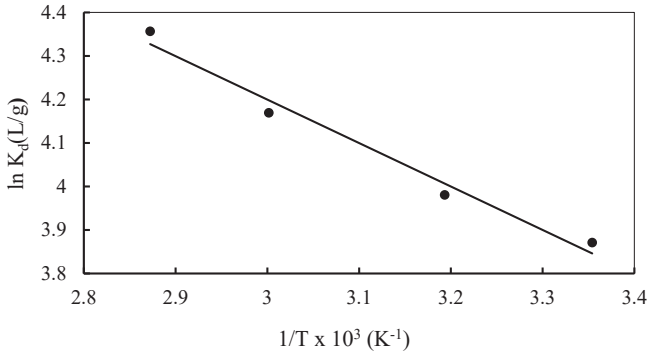

Fig. 11. Thermodynamic plot of Hg^{2+} adsorption onto (Ag/Q)NPs composite.

Table 4
Thermodynamic parameters for Hg^{2+} adsorption onto (Ag/Q)NPs composite.

Temperature (K)	ΔG (kJ/mol))	ΔH (kJ/mol)	ΔS (J/mol K)	R^2
313	-10.3	8.3	59.8	0.978
333	-11.5			
348	-12.6			

occurs due to close redox potentials of two metals. The mechanism also suppose the formation of an amalgam between two metals Ag_xHg_y or precipitation of Hg° on the composite surface. So the mechanism of Hg^{2+} removal might physical adsorption and/or precipitation of mercury as Hg°. Henglein and Brancewicz [60] and Henglein [61] observed the Hg^{2+} reduction and amalgamation according to the following reactions Hg^{2+} and Ag NPs:

$$Ag_m + (m/2)\ Hg^{2+} \rightarrow mAg^{+} + (m/2)\ Hg \quad (16)$$

$$Ag_n + Hg^{2+} \rightarrow Ag_{(n-2)}Hg + 2Ag^{+} \quad (17)$$

Additional studies are required to comprehend the Hg^{2+} removal mechanism and to assess the expenses and advantages of using quartz/Ag NPs nanocomposite materials.

3.3. Thermodynamic studies

Temperature-dependent adsorption isotherms (Eqs. (13), (14), and (15)) can be used to estimate the thermodynamic parameters (ΔH°, ΔS° and ΔG°) for Hg^{2+} ions adsorption on (Ag/Q)NPs composite nanoparticles. The values (ΔH°) and (ΔS°) can be predicted from the lnKd plot versus 1/T (Fig. 11). The positive (ΔH°) value indicates the process's endothermic nature. The free energy (ΔG°) of Hg^{2+} ions adsorption (Ag/Q)NPs is more negative at greater temperatures, which shows that the spontaneous nature of the adsorption method is more negative. The beneficial value of entropy change is due to the increased randomness of the solid-solution interface and a elevated mercury ion affinity (see Table 4).

3.4. Leaching and regeneration studies

Silver ions were leached slightly after 2hours using distilled water as the elluent. The leaching decreased with time and the release began to equilibrate at 12 hours with silver concentration of 0.01 mg/l (Fig. 12). Using HCl seems to be the highest eluent with an efficiency equal to 97% suggesting that (Ag/Q)NPs composite has a decent desorption capacity for Hg^{2+}. After four cycles of adsorption – desorption as shown in Fig. 13, the desorption capacity of the prepared composite slightly decreased. The release of Ag+ ions using HCl acid by desorption of Hg^{2+} was very low and can be ignored, which can help the adsorption of Hg^{2+} on the composite surface. The desorption of Hg^{2+} ions efficiency equal to 80 % using HNO_3 acid. The composite's reusability for Hg^{2+} adsorption was

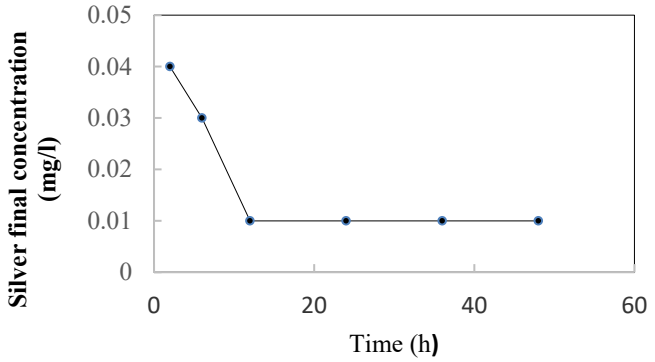

Fig. 12. Leaching test of Ag from (Ag/Q)NPs composite using distilled water.

reported at 95%, which before adsorption is almost the same. The (Ag/Q)NPs composite was therefore an effective and stable Hg^{2+} removal adsorbent. Due to adsorbent structural instability, the adsorption capacity may be decreased after regeneration.

3.5. Comparison with other studies

Many variables play a crucial role in the efficiency of adsorption capacity such as the origin of the adsorbent, the type of modification, metal ion solution experimental conditions (pH, ionic medium, ionic strength, metal ion concentration, temperature). This makes it hard to compare the adsorption capacity of the distinct adsorbents as it depends on the variables listed above. Table 5 shows the ranges of maximum adsorption capacity values (qm) of some adsorbents towards Hg^{2+} removal. As we observe in this work, composite (Ag/Q)NPs) removed 376.3 mg/g Hg^{2+} ions at pH 6 from the aqueous solution. This good result is ascribed to wealthy active adsorbent sites in (Ag/Q)NPs) composite, besides being non-toxic and having antibacterial activity [62]. The (Ag/Q)NPs) composite could therefore be one of the best candidates to remove mercury ions from water solution for drinking water preparation.

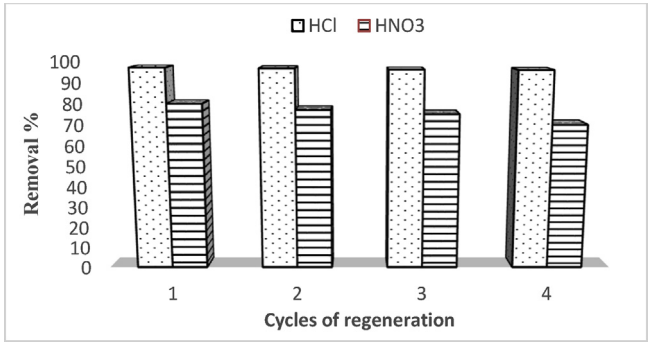

Fig. 13. Regeneration of Hg^{2+} ions from (Ag/Q)NPs composite.

Table 5
Ranges of maximum adsorption capacity values (qm) of some adsorbents towards Hg^{2+} removal.

Adsorbent	Maximum adsorption capacity (q_m)	Ref.
Ag supported on nano mesoporous silica.	42.26 mg/g	[55]
buckwheat hulls	243.90 mg/g	[63]
LCF wastes of coconut	144.4 mg/g	[64]
Apatite	38 mg/g	[65]
Hybrid nanoslica	134 mg/g	[66]
modified sodium montmorillonite	140.84 mg/g	[67]
Ag/quartz nanocomposite	376.3 mg/g	This work

4. Conclusion

In this study, natural quartz, silver nanoparticles AgNPs and Ag/quartz nanocomposite (Ag/Q)NPs)) were used as adsorbents to remove mercury ions from aqueous solution. AgNPs and (Ag/Q)NPs)) composite were synthesized by sol-gel method using table sugar as chelating agent. The prepared samples were characterized using XRD results emphasized the formation of (Ag/Q)NPs)) composite where AgNPs are embedded inside the quartz matrix. The BET surface area, the total pore volume and the porosity of the (Ag/Q)NPs)) composite are smaller than that obtained for the pure AgNPs and quartz. TEM of (Ag/Q)NPs)) composite confirmed that AgNPs not only located on the surface but also embedded within the matrix of quartz. Adsorption is strongly dependent on time, initial metal concentration, dose of adsorbent and initial pH. (Ag/Q)NPs)) composite yielded the maximum removal of mercury ions from the aqueous solution 96% at 60 min with 0.5g adsorbent dose at pH 6. The equilibrium adsorption isotherms are well fitted by Langmuir equations. The adsorption process followed the pseudo-second order model. Positive ΔH and ΔS values indicated that the adsorption of Hg^{2+} ions onto (Ag/Q)NPs)) composite was endothermic, spontaneous and feasible process.

Declarations

Author contribution statement

R. S. El-Tawil: Conceived and designed the experiments; Performed the experiments; Analyzed and interpreted the data; Contributed reagents, materials, analysis tools or data.

S. T. El-Wakee, A. E. Abdel-Ghany: Conceived and designed the experiments; Performed the experiments; Analyzed and interpreted the data.

H. A.M. Abuzeid: Conceived and designed the experiments; Performed the experiments.

K. A. Selim: Contributed reagents, materials, analysis tools or data.

A. M. Hashem: Analyzed and interpreted the data; Wrote the paper.

Funding statement

This work was partially funded by National Research Center, Cairo, Egypt through house project with ID (11050104).

Competing interest statement

The authors declare no conflict of interest.

Additional information

No additional information is available for this paper.

References

[1] S.K. Pradhana, J. Panwarb, S. Gupta, Enhanced heavy metal removal using silver-yttrium oxide nanocomposites as novel adsorbent system, J. Environ. Chem. Eng. 5 (2017) 5801–5814.

[2] R.G. Garriga, A.P. Foguet, Unravelling the linkages between water, sanitation, hygiene and rural poverty: the WASH poverty index, Water Resour. Manag. 27 (2013) 1501–1515.

[3] H.S. Samanta, R. Das, C. Bhattachajee, Influence of nanoparticles for wastewater treatment – a short review, Austin Chem. Eng. 3 (3) (2016) 1036.

[4] K.O. Shittu, O. Ihebunna, Purification of simulated waste water using green synthesized silver nanoparticles of Piliostigma thonningii aqueous leave extract, Adv. Nat. Sci. Nanosci. Nanotechnol. 8 (2017) 045003.

[5] A. Jada, R.A. Akbour, Adsorption and removal of organic dye at quartz sand-water interface adsorption et désorption d'un colorant organique à l'interface sable de quartz-eau, Oil & Gas Sci. & Techn. – Rev. IFP Energies nouvelles 3 (2014) 405–413.

[6] R.S. Dubey, R. Xavier, Study on removal of toxic metals using various adsorbents from aqueous environment: a review, Sci. J. Eng. 1 (1) (2015) 30–36.

[7] F. Ge, M.M. Li, H. Ye, B.X. Zhao, Effective removal of heavy metal ions Cd^{2+}, Zn^{2+}, Pb^{2+}, Cu^{2+} from aqueous solution by polymer-modified magnetic nanoparticles, J. Hazard. Mater. 211 (2012) 366–372.

[8] X. Wang, Y. Guo, L. Yang, M. Han, J. Zhao, X. Cheng, Nanomaterials as sorbents to remove heavy metal Ions in wastewater treatment, J. Environ. Anal. Toxicol. 2 (7) (2012) 1000154.

[9] L.M. Windham, J.A. Fleck, J.T. Ackerman, M.D. Marvin, C.A. Stricker, W.A. Heim, P.A.M. Bachand, C.A.S. Eagles, G. Gill, M. Stephenson, C.N. Alpers, Mercury cycling in agricultural and managed wetlands: a synthesis of methylmercury production, hydrologic export, and bioaccumulation from an integrated field study, Sci. Total Environ. 484 (2014) 221–231.

[10] S. Malar, S.V. Sahi, P.J.C. Favas, P. Venkatachalam, Mercury heavy-metal-induced physiochemical changes and genotoxic alterations in water hyacinths [*Eichhornia crassipes* (Mart.)], Environ. Sci. Pollut. Res. 22 (2015) 4597–4608.

[11] P. Miretzky, A.F. Cirelli, Hg(II) removal from water by chitosan and chitosan derivatives: a review, J. Hazard. Mater. 167 (2009) 10–23.

[12] H. Parham, B. Zargar, R. Shiralipour, Fast and efficient removal of mercury from water samples using magnetic iron oxide nanoparticles modified with 2-mercaptobenzothiazole, J. Hazard. Mater. 205 (2012) 94–100.

[13] A. Ali, A. Mannan, I. Hussain, M. Zia, Effective removal of metal ions from aquous solution by silver and zinc nanoparticles functionalized cellulose: isotherm, kinetics and statistical supposition of process, Environ. Nanotechnol. Monit. Manag. 9 (2018) 1–11.

[14] A. Pereira, A.F. Martins, A.T. Paulino, A.R. Fajardo, M.R. Guilherme, M.G.I. Faria, G.A. Linde, A.F. Rubira, E.C. Muniz, Recent advances in designing hydrogels from chitin and chitin-derivatives and their impact on environment and agriculture: a review, Virtual Quim. 9 (2017).

[15] I. Ali, V. Gupta, Advances in water treatment by adsorption technology, Nat. Protoc. 1 (6) (2016) 2661–2667.

[16] B. Pan, W. Zhang, Q. Zhang, S. Zhang, Development of polymeric and polymer-based hybrid adsorbents for pollutants removal from waters, Chem. Eng. J. 151 (2009) 19–29.

[17] G. Chauhan, P.U.K. Chauhan, Risk assessment of heavy metal toxicity through contaminated vegetables from waste, Int. J. Adv. Technol. Eng. Sci. 51 (2014) 444–460.

[18] O. Hakami, Y. Zhang, C.J. Banks, Thiol-functionalized mesoporous silica-coated magnetite nanoparticles for high efficiency removal and recovery of Hg from water, Water Res. 46 (2012) 3913–3922.

[19] B. Li, Y. Zhang, D. Ma, Z. Shi, S. Ma, Mercury nano-trap for effective and efficient removal of mercury (II) from aqueous solution, Nat. Commun. 5 (2014).

[20] M.K. Uddin, A review on the adsorption of heavy metals by clay minerals, with special focus on the past decade, Chem. Eng. J. 308 (2017) 438–462.

[21] K.K. Yee, N. Reimer, J. Liu, S.Y. Cheng, S.M. Yiu, J. Weber, N. Stock, Z.T. Xu, Effective mercury sorption by thiol-laced metal-organic frameworks: in strong acid and the vapor phase, J. Am. Chem. Soc. 135 (2013) 7795–7798.

[22] E.A. Kim, A.L. Seyfferth, S. Fendorf, R.G. Luthy, Immobilization of Hg(II) in water with polysulfide-rubber (PSR) polymer-coated activated carbon, Water Res. 45 (2011) 453–460.

[23] A. Gupta, S.R. Vidyarthi, N. Sankararamakrishnan, Enhanced sorption of mercury from compact fluorescent bulbs and contaminated water streams using functionalized multiwalled carbon nanotubes, J. Hazard. Mater. 274 (2014) 132–144.

[24] Khairia M. Al-Qahtani, Cadmium removal from aqueous solution by green synthesis zero valent silver nanoparticles with Benjamina leaves extract, Egypt. J. Aqua. Res. 43 (2017) 269–274.

[25] Y. Zhang, B. Wu, H. Xu, H. Liu, M. Wang, Y. He, B. Pan, Nanomaterials-enabled water and wastewater treatment, Nano Impact 3 (4) (2016) 22–39.

[26] X.F. Ma, Y.Q. Wang, M.J. Gao, H.Z. Xu, G.A. Li, A novel strategy to prepare ZnO/PbS hetero structured functional nanocomposite utilizing the surface adsorption property of ZnO nanosheets, Catal. Today 158 (2010) 459–463.

[27] S.T. El-Wakeel, R.S. El-Tawil, H.A.M. Abuzeid, A.E. Abdel-Ghany, A.M. Hashem, Synthesis and structural properties of MnO_2 as adsorbent for the removal of lead (Pb^{2+}) from aqueous solution Synthesis and structural properties of MnO_2 as adsorbent for the removal of lead (Pb^{2+}) from aqueous solution, J. Taiwan Inst. Chem. Eng. 72 (2017) 95–103.

[28] S.G. Kim, N. Hagura, F. Iskandar, K. Okuyama, Characterization of silica-coated Ag nanoparticles synthesized using a water-soluble nanoparticle micelle, Adv. Powder Tech. 20 (2009) 94–100.

[29] E. Vélez, G.E. Campillo, G. Morales, C. Hincapié, J. Osorio, O. Arnache, J.I. Uribe, F. Jaramillo, Mercury removal in wastewater by iron oxide nanoparticles, J. Phys. C 687 (1) (2016) 012050.

[30] Y. Xie, B. Yan, C. Tian, Y. Liu, Q. Liu, H. Zeng, Efficient removal of elemental mercury (Hg0) by SBA-15-Ag adsorbents, J. Mater. Chem. A2 (2014) 17730.

[31] E. Sumesh, M.S. Bootharaju, T. Anshup, A. Pradeep, Practical silver nanoparticlebased adsorbent for the removal of Hg^{2+} from water, J. Hazard. Mater. 189 (2011) 450–457.

[32] J. Theron, J.A. Walker, T.E. Cloete, Nanotechnology and water treatment: applications and emerging opportunities, Crit. Rev. Microbiol. 34 (2008) 43–69.

[33] P. Amornpitoksuk, S. Suwanboon, S. Sangkanu, A. Sukhoom, N. Muensit, J. Baltrusaitis, Synthesis, characterization, photocatalytic and antibacterial activities of Ag-doped ZnO powders modified with a diblock copolymer, Powder Technol. 219 (2012) 158–164.

[34] B. Sun, S. Sun, T. Li, W. Zhang, Preparation and antibacterial activities of Ag-doped SiO_2–TiO_2 composite films by liquid phase deposition (LPD) method, J. Mater. Sci. 42 (2007) 10085–10089.

[35] N. Sobana, M. Muruganadham, M. Swaminathan, Nano-Ag particles doped TiO_2 for efficient photodegradation of direct azo dyes, J. Mol. Catal. A Chem. 258 (2006) 124–132.

[36] M. Kawashita, S. Tsuneyama, F. Miyaji, T. Kokubo, H. Kozuka, K. Yamamoto, Antibacterial silver-containing silica glass prepared by sol-gel method, Biomaterials 21 (2000) 393–398.

[37] C. Racles, A. Nistor, M. Cazacu, A silica-silver nanocomposite obtained by sol-gel method in the presence of silver nanoparticles, Cent. Eur. J. Chem. 11 (10) (2013) 1689–1698.

[38] A.M.E. Marchand, R.S. Haszeldine, C.I. Macaulay, R. Swennen, A.E. Fallick, Quartz ementation inhibited by crestal oil charge: miller deep water sandstone, UK North Sea, Clay Miner. 35 (2016), 201–201.

[39] A. Jada, R.A. Akbour, Adsorption and removal of organic dye at quartz sand-water interface, Oil & Gas Sci. and Tech. – Rev. IFP. Energies nouvelles 69 (3) (May–June 2014).

[40] H.M.F. Freundlich, Over the adsorption in solution, J. Phys. Chem. 57 (1906) 385–470.

[41] I. Langmuir, The adsorption of gases on plane surfaces of glass, mica and platinum, J. Am. Chem. Soc. 40 (1918) 1361–1403.

[42] M.M. Dubinin, L.V. Radushkevich, Equation of the characteristic curve of activated charcoal, Proc. Acad. Sci. USSR Phys. Chem. Sect. 55 (1) (1947) 331–337.

[43] O. Redlich, D.L. Peterson, A useful adsorption isotherm, J. Phys. Chem. 63 (1959) 1024–1026.

[44] Y.S. Ho, Citation review of Lagergren kinetic rate equation on adsorption reactions, Scientometrics 59 (2004) 171–177.

[45] Y.S. Ho, Review of second-order models for adsorption systems, J. Hazard. Mater. 136 (2006) 681–689.

[46] T.W. Weber, R.K. Chakravorti, Pore and solid diffusion models for fixed-bed adsorbers, AIChE J. 20 (1974) 228–238.

[47] J.W.J. Weber, J.C. Morris, J. Sanit, Kinetics of adsorption on carbon from solution engineering division, Am. Soc. Civil Eng. 89 (1963) 31–38.

[48] S.I. Lyubchik, A.I. Lyubchik, O.L. Galushko, L.P. Tikhonova, J. Vital, I.M. Fonseca, S.B. Lyubchik, Kinetics and thermodynamics of the Cr (III) adsorption on the activated carbon from co-mingled wastes, Colloid. Surf. A Physicochem. Eng. Asp. 242 (2004) 151–158.

[49] K. Dudek, J. Podwórny, M. Dulski, A. Nowak, J. Peszke, X-ray investigations into silica/silver nanocomposite, Powder Diffr. J. 32 (2017) S82–S86.

[50] K. Toisawa, Y. Hayashi, H. Takizawa, Synthesis of highly concentrated Ag nanoparticles in a heterogeneous solid-liquid system under ultrasonic irradiation, Mater. Trans. 51 (10) (2010) 1764.

[51] L.H. Chou, I.C. Chung, P.Y. Hsu, Proceedings of SPIE, SPIE, Bellingham, WA, 2005, p. 5643.

[52] S.J. Gregg, K.S.W. Sing, Adsorption, Surface Area, and Porosity, 2nd ed, Academic Press, London, 1982.

[53] IUPAC recommendations, Pure Appl. Chem. 66 (1994) 1739.

[54] P. Yuan, D. Liu, M.D. Fan, D. Yang, R.L. Zhu, Removal of hexavalent chromium [Cr(VI)] from aqueous solutions by the diatomite-supported/unsupported magnetite nanoparticles, J. Hazard. Mater. 173 (2010) 614–621.

[55] M.A.A. Ganzagh, M. Yousef, Z. Taherian, The removal of mercury (II) from water by Ag supported on nanomesoporous silica, J. Chem. Biol. 9 (2016) 127–142.

[56] K.R. Hall, L.C. Eagleton, A. Acrivos, T. Vermeulen, Pore- and solid-diffusion kinetics in fixed-bed adsorption under constant-pattern conditions, Ind. Eng. Chem. Fundam. 5 (1966) 212.

[57] N. Asasian, T. Kaghazchi, Optimization of activated carbon sulfurization to reach adsorbent with the highest capacity for mercury adsorption, Sep. Sci. Technol. 48 (2013) 2059–2072.

[58] C.J. Aguilar, F. Garrido, L. Barrios, G.M.T. Garcia, Sorption of As, Cd and Tl as influenced by industrial by-products applied to an acidic soil: equilibrium and kinetic experiments, Chemosphere 65 (2006) 2377–2387.

[59] Z. Tauanov, P.E. Tsakiridis, S.V. Mikhalovsky, V.J. Inglezakis, Synthetic coal fly ash-derived zeolites doped with silver nanoparticles for mercury (II) removal from water, J. Environ. Manag. 224 (2018) 164–171.

[60] A. Henglein, C. Brancewicz, Absorption spectra and reactions of colloidal bimetallic nanoparticles containing mercury, Chem. Mater. 4756 (1997) 2164–2167.

[61] A. Henglein, Colloidal silver nanoparticles: photochemical preparation and interaction with O_2, CCl_4, and some metal ions, Chem. Mater. 2 (1998) 444–450.

[62] H. Xuanmeng, F. Wang, H. Liu, J. Li, L. Niu, Synthesis of quartz crystals supporting Ag nanoparticle powder with enhanced antibacterial properties, Surf. Interfaces 6 (2017) 122–126.

[63] Z.D. Wang, P. Yin, R.J. Qu, H. Chen, C.H. Wang, S.H. Ren, Adsorption kinetics, thermodynamics and isotherm of Hg(II) from aqueous solutions using buckwheat hulls from Jiaodong of China, Food Chem. 136 (2013) 1508–1514.

[64] K. Johari, N. Saman, S.T. Song, J.Y.Y. Heng, H. Mat, Study of Hg(II) removal from aqueous solution using lignocellulosic coconut fiber biosorbents: equilibrium and kinetic evaluation, Chem. Eng. Commun. 201 (2014) 1198–1220.

[65] J. Oliva, J. De Pablo, J.L. Cortina, J. Cama, C. Ayora, Removal of cadmium, copper, nickel, cobalt and mercury from water by Apatite II™: column experiments, J. Hazard Mater. 194 (2011) 312–323.

[66] D.P. Quintanilla, I. Sierra, Factors affecting Hg(II) adsorption on hybrid nanostructured silicas: influence of the synthesis conditions, J. Porous Mater. 21 (2014) 71–80.

[67] A.S.K. Kumar, S. Kalidhasan, V. Rajesh, N. Rajesh, A meticulous study on the adsorption of mercury as tetrachloromercurate(II) anion with trioctylamine modified sodium montmorillonite and its application to a coal fly ash sample, Ind. Eng. Chem. Res. 51 (2012) 11312–11327.